

## Transient shear banding of complex fluids

Antti Puisto, Xavier Illa, Arttu Lehtinen, Mikael Mohtaschemi, and Mikko Alava

Aalto University, School of Science, Department of Applied Physics,  
P.O. Box 14100, FI-00076 AALTO, Finland

### ABSTRACT

We discuss recent models on the dynamics of shear band formation and transient shear banding. The approach here is that of simple rheology, which describe the structure of the complex fluid's internal phase using a relaxation kinetics equation. This way, the structure of the fluid is described in the simplest case using a single parameter. The state of the structure, in turn, is mapped to the continuum characteristics of the fluid via the appropriate constitutive equations giving the possibility to simulate the fluid rheology. Coupling these models with a continuum description of the flow field, allows for studying spatial and temporal flow heterogeneities, for instance shear banding. Here we consider in detail the evolutions of velocity and shear rate profiles in the Couette geometry during a start-up phase, experimentally demonstrated to show transient shear banding even in materials shown to possess monotonous flow curves. Using this simple approach we find that the underlying reason for such start-up instabilities is the non-homogeneous shear distribution, which is amplified due to a positive feedback between the flow field and the viscosity response of the time-dependent fluid. As we will demonstrate, this offers a simple explanation for the recent observations of Transient Shear Banding not only limited to simple yield stress fluids.

### INTRODUCTION

The characteristic property of complex fluids is their non-linear shear rate – stress

relation called the flow curve. These materials are generally formed of an internal, structure forming phase surrounded by a dispersing liquid medium.<sup>1</sup> Such complex fluids can have states resembling both, solid and liquid states.<sup>2</sup> Obviously, their characteristics can lead to highly non-trivial flow behaviors such as shear banding and rheo-chaos<sup>3</sup>.

In shear thinning fluids, such as some aggregating colloids, emulsions, and microgels, the structure usually gets less organized at higher shear rates, and at vanishing shear rates, a space filling internal structure is formed<sup>4</sup> leading to a dynamical arrest at vanishing shear rates.<sup>5</sup> This space filling structure, is responsible for the materials solid-like properties, such as its ability to support load, i.e. yield stress.<sup>6</sup> While in some materials, this structure can also evolve without the presence of external stress, modifying the yield stress, in others, no evidence of this kind of *ageing* is observed. This has led to the crude categorization of complex fluids into thixotropic, and simple fluids.<sup>7</sup> Apparently also the simple fluids show time-dependent properties, in a less pronounced way, however.<sup>8</sup> What remained clear, was that shear banding was only observed in the thixotropic fluids, and not in the simple ones. This was thought to be related to the shape of the intrinsic flow curve in each case.

Recently, a different type of shear banding was observed also in the simple yield stress fluids.<sup>9</sup> Due to its appearance only during the start-up phase, this was called transient shear banding. At first sight, this

seemingly contradicted the present understanding for the reasons of shear banding. The main issue was that since these simple yield stress fluids do not have non-monotonic flow curves, how is it possible for them to shear band at all. Furthermore, this type of shear banding or gradual fluidization was observed to show characteristics typically seen in phase transitions, for instance critical scaling for the fluidization times with both imposed strain rate and stress. This hinted to the possibility of probing the time-scales related to the fluid relaxation, giving the possibility to find models beyond the steady state ones for obtaining deeper understanding of the yielding process.

In this paper we review our modeling work performed to understand the start-up flows that seem to imply a new way of probing the yielding transition in complex fluids. We address the related open issues using simple scalar  $\lambda$ -models, trying to understand if the critical scaling, and the related exponents could be due to the material, or the experimental setting, or possibly, both. The rest of the paper is organized such that first, we give an overview of the models applied, then we will discuss in detail the transient behavior of the flow profiles and the related stress over-shoots in the light of related experiments, and finally, we make some conclusions, and discuss on the related open questions.

## MODEL

We start by describing the evolution of the fluids internal structure described using a scalar parameter  $\lambda$ . The time evolution of this parameter is given by<sup>10</sup>

$$\frac{d\lambda}{dt} = \frac{1}{\tau} - \alpha\dot{\gamma}\lambda, \quad (1)$$

where  $\tau$  is the characteristic timescale for the structure build-up, and  $\alpha$  is the scale of the structure destruction due to shear. The internal structure parameter relates to the viscosity of the fluid via a simple linear equation, which reads

$$\eta(\lambda) = \eta_0 (1 + \beta\lambda^n). \quad (2)$$

There,  $\eta_0$  is the liquid viscosity, and  $\beta$  and  $n$  are material dependent parameters, the latter controlling the linearity of the viscosity function with respect to  $\lambda$ . From

this equation it follows, that at  $\lambda = 0$ , where the structure is completely broken, the fluid has the viscosity of the surrounding medium, whereas when  $\lambda \rightarrow \infty$ , the structure approaches complete, also the viscosity diverges. Given the stress consists only of the viscous one ( $\sigma = \dot{\gamma}\eta$ ), later referred to as the *viscous model* the yield stress can be written as

$$\sigma_y = \frac{\beta}{\tau\alpha}. \quad (3)$$

The steady state of such simple phenomenological model captures the behaviors of shear thinning ( $n < 1$ ), simple yield stress ( $n = 1$ ), as well as thixotropic fluids ( $n > 1$ ) as discussed in earlier studies<sup>10</sup> and demonstrated in Fig. 1.

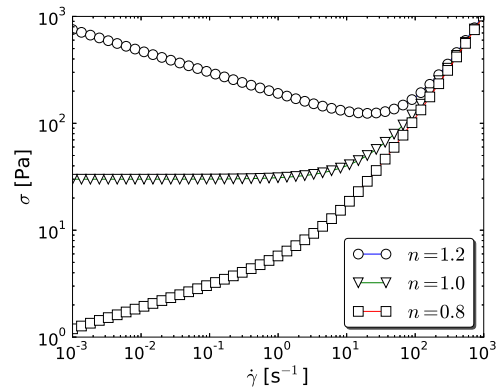


Figure 1. The steady state of the model showing shear thinning, simple yield stress, and thixotropic behaviors.

In real materials, the stress has in general both viscous and elastic components. Elastic stress can be incorporated to the previous fluid model by taking the constitutive relation of a Maxwell stress element instead of the viscous one<sup>11</sup>. Now the stress equation reads<sup>12</sup>

$$\sigma = \eta(\lambda)\dot{\gamma} - \frac{\eta(\lambda)}{G_0} \frac{\partial \sigma}{\partial t} \quad (4)$$

where  $G_0$  is the shear modulus. Here, the stress consists additionally to a viscous term, with an elastic term, which is proportional to the rate at which the stress changes and the inverse of the systems elastic modulus. This implies that fast transitions in the stress first cause loading of the

elastic stress, which then relaxes through viscous dissipation. Later in the text this will be referred to as the *elastic model*. Clearly, this definition of stress only has an influence during the shear transients, and therefore, the steady state of the viscous and elastic models are the same.

In shear banding, the shear rate and viscosity vary over a spatial coordinate of the system considered. To model such effects, we solve the structural model in conjunction with the Navier-Stokes equation evolving a separate structural model locally. For the Navier-Stokes equation, we apply the boundary conditions of cylindrical Couette geometry in order to be able to compare the results with recent experimental data obtained for simple yield stress fluids.<sup>9</sup> These boundary conditions give for the local shear rate

$$\dot{\gamma}(r) = \frac{\Omega_b - \Omega_a}{r^2 \eta(r) \int_{R_a}^{R_b} \frac{1}{r^3 \eta(r)} dr}, \quad (5)$$

where  $r$  is the radial position measured from the Couette center,  $\Omega_a$  ( $\Omega_b$ ) is the angular velocity of the inner (outer) cylinder, and  $R_a$  ( $R_b$ ) is the radius of the inner (outer) cylinder. In these simulations we apply  $R_a = 2.39$  cm and  $R_b = 2.50$  cm which are typical values for a narrow gap Couette device and similar to the geometry used in the first observations of transient shear banding in carbopol gels<sup>13</sup>. Moreover, we keep the outer cylinder fixed, while controlling the angular velocity of the inner cylinder to fix either the global shear rate given by

$$\langle \dot{\gamma} \rangle = (\Omega_b - \Omega_a) \frac{2R_a R_b}{R_b^2 - R_a^2}, \quad (6)$$

or the stress at the inner cylinder, depending on the driving mode. To solve the time evolution, we discretize the gap ( $r$ ) in 450 equally dimensioned shells. We integrate the thus formed set of differential equations using the SUNDIALS CVODE solver routines.<sup>14</sup>

## RESULTS

In the start-up experiments, the samples are initially under no shear, having solid-like properties. This, in terms of the structural model, means that the structure is maximally organized, in the present

model implying  $\lambda_0 \rightarrow \infty$ . Since in the simulations we are bounded by the floating point range, we initialize the system to a high viscosity state, where  $\lambda_0$  is large, but finite. This implies that the system is always in a flowing state, and the liquid-solid phase transition is completely absent. Similarly to the experiments, we start the flow at  $t = 0$  and observe the local shear rate and velocity behaviors. In the viscous model, we find that after a short initial induction period having linear velocity profile, the shear localizes gradually right next to the rotor, as visualized in Fig 2. Such process occurs rather quickly, here in a matter of a few seconds. This localization could in practice be confused with wall slip, however, in the present model, the boundary conditions fix the fluid velocity at the wall, and therefore this localization is simply a structural property of the fluid. This shows that for fluids having time-dependent shear thinning properties, this kind of behavior is intrinsic to the fluid, and can not be avoided by any of the traditional methods of avoiding wall slip.<sup>15</sup>

After the shear is almost completely localized at the rotor, the high shear regime starts to grow due to the delayed relaxation of the quiescent band into a full blown high shear band, which gradually continues to advance towards the rotor. Finally, once the steady state is reached in the whole geometry, the shear band has reached the stator. A typical example of such relaxation process is shown in Fig. 3.

Although, this relaxation process resembles quite closely the transient shear bands experimentally observed in carbopol gels,<sup>9</sup> there are some differences. For instance, the experiments find elastic backward flows when the "wall slip" appears. Moreover, they find slowly building stress over-shoots, which do not comply with a purely viscous model. Finally, during the relaxation period, the shear rate in the whole quiescent band seems to increase simultaneously with the shear band edge movement in the radial direction.<sup>16</sup>

The start-up flow results of the elastic model follow those of the viscous one until the shear begins to localize near the rotor<sup>11</sup>. When the localization of the shear starts, an elastic backward flow appears, during which the high shear band begins

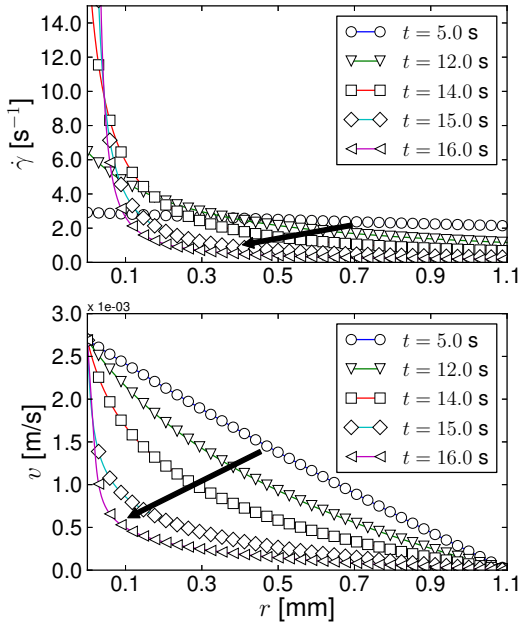


Figure 2. Initial stage of the transient shear band in the Couette gap. Plotted are the shear rate (upper panel) and the corresponding velocity (lower panel) profiles. The applied simulation parameters are  $\alpha = 0.1$ ,  $\tau = 0.001$ ,  $\eta_0 = 1.0$ ,  $\beta = 0.003$ ,  $\lambda_0 = 2.5 \cdot 10^6$ , and  $\langle \dot{\gamma} \rangle = 2.5 \text{ s}^{-1}$ .

to form. Despite the fact that the elastic backwards flow appears very quickly, the overall time for the shear localization is longer for the viscoelastic fluid compared to the viscous one.

The transient shear band relaxation for the viscoelastic model, reported in Fig. 5, also differs from the viscous case. Here, the shear bands relax rather in a collective manner, than via a moving boundary; the shear rate in the quiescent band increases simultaneously to the decrease of the shear rate in the highly sheared band. This agrees with the experimental observation, that the quiescent band is not completely static, but evolves throughout the fluidization.

The stress evolution curves plotted for the viscoelastic case in Fig. 6 show stress over-shoots, the magnitude of which de-

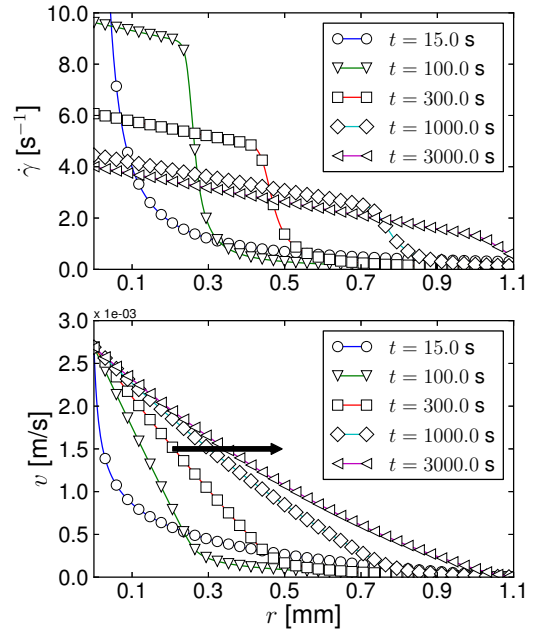


Figure 3. Shear band relaxation in the Couette gap. The simulation parameters are the same as in Fig. 2.

pends on the  $\lambda_0$ . The stress first increases due to the elastic loading of the system. After the stress maximum, the viscous dissipation starts to play a significant role as the structure is more broken at the rotor. At the same time, when the stress drops, an elastic backward flow is observed in the velocity profiles, which creates the transient shear band. Once the transient shear band is created, the stress relaxation slows down, and starts decreasing with a completely different slope. Thus, the existence of the transient shear band can also be observed in the stress evolution curves, again, in agreement with the carbopol experiments<sup>16</sup>. As can be seen in the figure, the over-shoot gets smaller with decreasing  $\lambda_0$ . Similarly, the transient shear bands get less and less pronounced, and finally do not appear at all in the case where the over-shoot is non-existent. Such dependence on the initial structure is sensible also in the practical viewpoint, indicating that the history of the sample influences the stress over-shoot. The more the sample is pre-sheared, and the less time is left

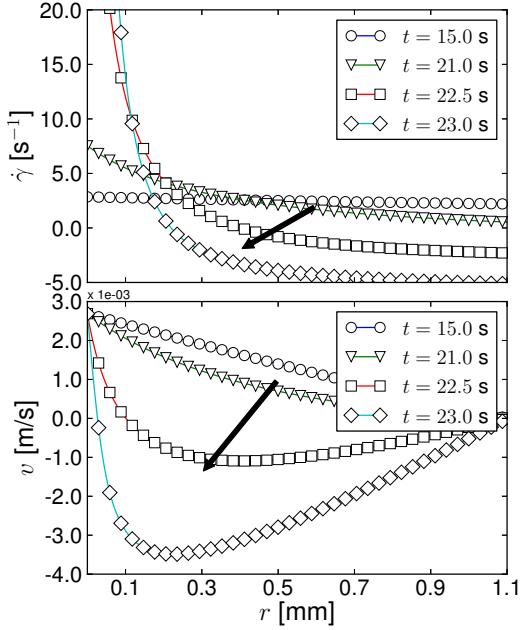


Figure 4. Shear band formation in the Couette gap for the viscoelastic stress model. Plotted are the shear rate (upper panel) and the corresponding velocity (lower panel) profiles. To produce the figures we applied  $\alpha = 0.1$ ,  $\tau = 0.001$ ,  $\eta_0 = 1.0$ ,  $\beta = 0.003$ ,  $G_0 = 5.0$ ,  $\lambda_0 = 2.5 \cdot 10^6$ , and  $\langle \dot{\gamma} \rangle = 2.5 \text{ s}^{-1}$ .

for recovery, the smaller is the stress overshoot.

The transient shear band life-times, the fluidization times, can be measured from these systems by tracking the shear band edge location in the gap. Experimentally, the fluidization time was observed to scale according to a power-law with respect to both, the global shear rate, and with the imposed (reduced) stress.<sup>9</sup> In these models we trace the shear band edge by following the position of the maximum of the shear rate's spatial derivative,  $\delta := \max \left[ \frac{\partial \dot{\gamma}(r,t)}{\partial r} \right]$ , where the discontinuous transition between the two shear rates occurs. Once the position of this quantity reaches either edge of the simulation grid, the system is defined as fluidized. Tracing the fluidization times in both the viscous and viscoelas-

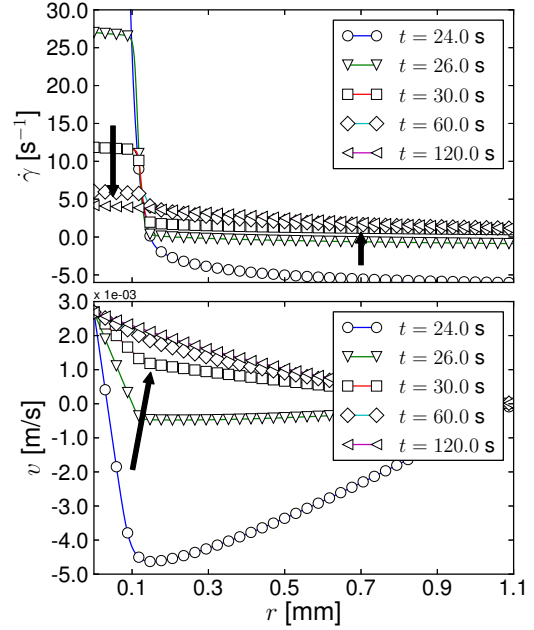


Figure 5. Shear band relaxation in the Couette gap for the viscoelastic stress model. The same parameters as in Fig. 4 are applied.

tic models gives the fluidization time a power-law like dependence with both, the global shear rate (Fig. 7), and the reduced stress (Fig. 8). In the shear rate controlled case, the power-law scaling applies only at high shear rates due to an effect called the shear localization.<sup>17</sup> This is related to the plateau of the flow curve at small shear rates, which is more pronounced in the model compared to the carbopol, which causes a more pronounced shear rate variation in the Couette at small global shear rates. This prevents complete fluidization at small imposed global shear rates, and therefore, makes the fluidization times diverge. However, the exponents of these power-laws differ from the carbopol experiments<sup>9</sup>, here, having the values close to  $-1$  in all the cases, and in the experiments close to  $-2$  and  $-4$  for the shear rate controlled and stress controlled cases, respectively. In one of our papers,<sup>18</sup> we demonstrated, how these exponents are determined by the structural kinetics equation, and in particular, the dependence of the

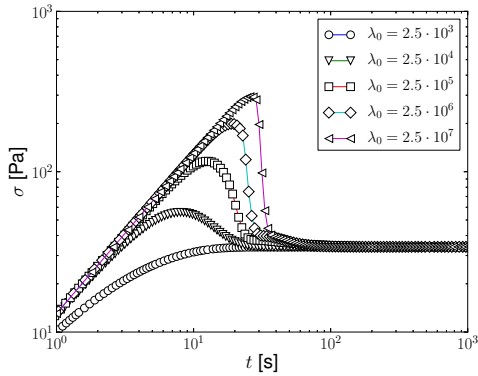


Figure 6. Stress over-shoots in the viscoelastic model with different initial structural parameters. The to produce the figure, we applied  $\alpha = 0.1$ ,  $\tau = 0.001$ ,  $\eta_0 = 1.0$ ,  $\beta = 0.003$ ,  $G_0 = 5.0$ , and  $\langle \dot{\gamma} \rangle = 2.5 \text{ s}^{-1}$ .

structure break-down term on the shear rate. We showed, that changing this particular exponent, the power-law fluidization time scaling exponents can be tuned. However, still, both the stress and shear rate controlled cases had the same exponents. Same holds for the models we have discussed here.

Based on experimental findings, the two fluidization times are proposed to be related with the steady state Herschel-Bulkley model

$$\sigma = \sigma_c + A\dot{\gamma}^k, \quad (7)$$

such that the Herschel-Bulkley exponent would be given by the two scaling exponent as  $k = \frac{a}{b}$ , where  $a$  is the one corresponding to the shear rate controlled fluidization, and  $b$  is the one corresponding to the stress controlled fluidization. Such relation comes out in a trivially from these simulations, since, as in the high shear rates the viscosity saturates to  $\eta_0$ , the stress scales as  $\sigma \sim \dot{\gamma}$ , the Herschel-Bulkley exponent is 1. Hence for this relation, we find  $\frac{1}{1} = 1$  for all the models (roughly for the elastic model). Thus, this trivial relation leaves the experimental observation unconfirmed.

## CONCLUSIONS

We have reviewed recent studies of transient shear banding. These were

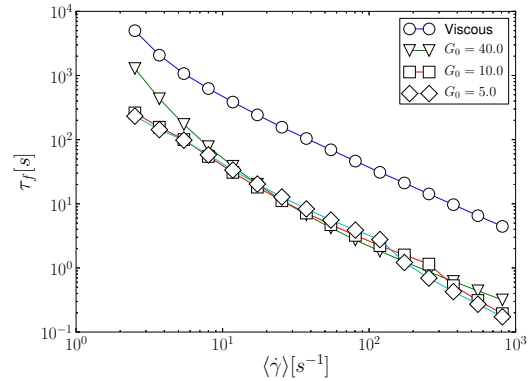


Figure 7. Fluidization times show a rough a power-law dependence with the global shear rate in the large shear rates, whereas at small shear rates they diverge due to shear localization. The simulation parameters  $\alpha = 0.1$ ,  $\tau = 0.001$ ,  $\eta_0 = 1.0$ ,  $\beta = 0.003$ , and  $\lambda_0 = 2.5 \cdot 10^6$  are applied.

first experimentally observed in a Couette rheometer in in carbopol gels<sup>9</sup>, known as a typical example of simple yield stress fluids, but since then also in aging soft glassy materials.<sup>19</sup> We demonstrated, how these non-homogeneous start-up flows, could be explained by the geometry induced shear inhomogeneity, which is amplified by the fluid relaxation. We showed, how many of the features, such as the relaxation paths are reproduced by the models, but also some open questions have been left unexplained. The most crucial one is the origins of the different fluidization time scalings of the shear rate and stress controlled experiments. It can be speculated, that since here we use a Maxwell stress model, it cannot well describe the creep-like features related to the stress controlled runs during the yielding phase. This has a direct implication, that adding a Kelvin-Voigt type of stress element to the Maxwell model could resolve these issues.

Furthermore, similar flow instabilities related to the start-up flow have been also reported with cone-and-plate geometry. At first thought, this particular geometry should impose a homogenous stress distribution, and therefore should not have similar mechanism for the shear band formation. However, even in such devices the stress varies slightly, which due to the fact

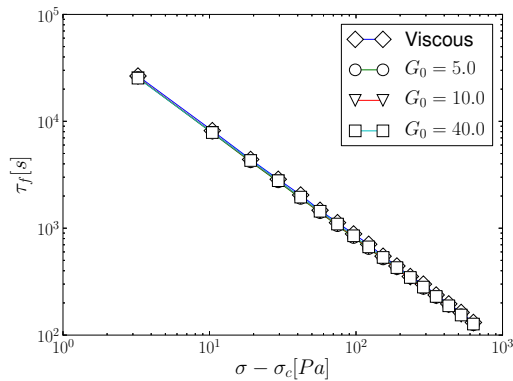


Figure 8. Fluidization times scale as a power-law with the reduced stress in the stress controlled simulations. For simulating the data, same parameters as in for Fig. 7 are used.

that the shear thinning tends to amplify the stress variations, can in fact lead to similar behavior. Moreover, the structure contact with the walls is even in those cases imperfect, which can initiate the flow instability.

#### ACKNOWLEDGEMENTS

This work was supported by the Effnet program in the Finnish Forest Cluster Ltd, and EU framework 7 program SUNPAP. Also, the support from the Academy of Finland through the COMP center of excellence, the project number 140268 and within the framework of the International Doctoral Programme in Bioproducts Technology (PaPSaT) are acknowledged.

#### REFERENCES

1. Berli, C.L.A. and Quemada, D. (2000). “Rheological Modeling of Microgel Suspensions Involving Solid-Liquid Transition”. *Langmuir*, **16**, 7968–7974.
2. Møller, P.C.F., Fall, A., and Bonn, D. (2009). “Origin of apparent viscosity in yield stress fluids below yielding”. *Eur. Phys. Lett.*, **87**, 38004.
3. Fielding, S.M. and Olmsted, P.D. (2004). “Spatiotemporal Oscillations and Rheochaos in a Simple Model of Shear Banding”. *Phys. Rev. Lett.*, **92**, 084502.
4. Barthelmes, G., Pratsinis, S., and Bugisch, H. (2003). “Particle size distribu-

tions and viscosity of suspensions undergoing shear-induced coagulation and fragmentation”. *Chemical Engineering Science*, **58**, 2893–2902. ISSN 00092509. doi: 10.1016/S0009-2509(03)00133-7.

5. Biroli, G. (2007). “A new kind of phase transition?” *Nature Phys.*, **3**, 222–223.
6. Coussot, P., Roussel, N., Jarny, S., and Chanson, H. (2005). “Continuous or catastrophic solid-liquid transition in jammed systems”. *Phys. Fluids*, **17**, 011704. ISSN 10706631. doi: 10.1063/1.1823531.
7. Møller, P., Fall, A., Chikkadi, V., Derks, D., and Bonn, D. (2009). “An attempt to categorize yield stress fluid behaviour”. *Phil. Trans. R. Soc. A*, **367**, 5139–5155.
8. Divoux, T., Grenard, V., and Manneville, S. (2013). “Rheological hysteresis in soft glassy materials”. *Phys. Rev. Lett.*, **110**, 018304.
9. Divoux, T., Tamarit, D., Barentin, C., and Manneville, S. (2010). “Transient Shear Banding in a Simple Yield Stress Fluid”. *Phys. Rev. Lett.*, **104**, 208301. doi: 10.1103/PhysRevLett.104.208301.
10. Møller, P.C.F., Mewis, J., and Bonn, D. (2006). “Yield stress and thixotropy: on the difficulty of measuring yield stresses in practice”. *Soft Matter*, **2**, 274.
11. Lehtinen, A., Puisto, A., Illa, X., Mohtaschemi, M., and Alava, M.J. “Transient shear banding of Maxwell fluids”. *Submitted*.
12. Lai, W., Rubin, D., and Krepl, E. (1999). *Introduction to continuum mechanics*. Butterworth-Heinemann.
13. Divoux, T., Tamarit, D., Barentin, C., Teitel, S., and Manneville, S. (2012). “Yielding dynamics of a Herschel-Bulkley fluid: a critical-like fluidization behaviour”. *Soft Matter*, **8**, 4151. ISSN 1744-683X. doi: 10.1039/c2sm06918k.
14. Cohen, S.D. and Hindmarsh, A.C. (1996). “CVODE, A stiff/nonstiff ode solver in C”. *Comp. Phys.*, **10**, 138.
15. Buscall, R. (2010). “Letter to the Editor: Wall slip in dispersion rheometry”. *J. Rheol.*, **54**, 1177.
16. Divoux, T., Barentin, C., and Manneville, S. (2011). “From stress-induced fluidization processes to Herschel-Bulkley behaviour in simple

yield stress fluids”. *Soft Matter*, **7**, 8409. ISSN 1744-683X. doi:10.1039/c1sm05607g.

17. Ovarlez, G., Rodts, S., Chateau, X., and Coussot, P. (2009). “Phenomenology and physical origin of shear localization and shear banding in complex fluids”. *Rheol. Acta*, **48**, 831.
18. Illa, X., Puisto, A., Lehtinen, A., Mohtaschemi, M., and Alava, M.J. (2013). “Transient shear banding in time-dependent fluids”. *Phys. Rev. E*, **87**, 022307.
19. Martin, J.D. and Hu, Y.T. (2012). “Transient and steady-state shear banding in aging soft glassy materials”. *Soft Matter*, **8**, 6940.